Vibratory Response Modeling and Verification of a High-Precision Optical Positioning System

Juan Barraza[a], Deming Shu[a], Tuncer Kuzay[a], and Thomas J. Royston[b]

[a]Argonne National Laboratory, 9700 S. Cass Avenue, Argonne, IL 60439

[b]Department of Mechanical Engineering, University of Illinois at Chicago, Chicago, IL 60607

ABSTRACT

A generic vibratory-response modeling program has been developed as a tool for designing high-precision optical positioning systems. Based on multibody dynamics theory, the system is modeled as rigid-body structures connected by linear elastic elements, such as complex actuators and bearings. The full dynamic properties of each element are determined experimentally or theoretically, then integrated into the program as inertial and stiffness matrices. Utilizing this program, the theoretical and experimental verification of the vibratory behavior of a double-multilayer monochromator support and positioning system is presented. Results of parametric design studies that investigate the influence of support floor dynamics and highlight important design issues are also presented. Overall, good matches between theory and experiment demonstrate the effectiveness of the program as a dynamic modeling tool.

Keywords: Vibration isolation, positioning stability, vibratory-response modeling

1. INTRODUCTION

At the Advanced Photon Source (APS), a third-generation 7-GeV synchrotron radiation facility at Argonne National Laboratory, high-precision positioning of large-scale optical devices is critical for achieving successful experiments. Optical instruments, such as mirrors, slits, and monochromators, principally rely on precision actuators for focusing, positioning, slitting, and/or tuning X-ray beams to micron-size dimensions and to meV energies. The large mass of each system, on the order of 1000 kg, and the need for positioning versatility and precision present a challenge to the vibration stability of the supporting structures and to the design of the positioning actuators. Potential vibration excitation sources at the APS site include ambient ground motion from seismic activity or machine or human activity in or near the experimental facility. Also, certain applications may include an excitation source as part of the optical system itself, such as cooling flow through optical components that interact with the beam.

In an effort to predict the vibratory response of optical positioning systems during their design, a modeling program has been developed by Basdogan[1] that is based on the theory of multibody dynamics. The model consists of lumped body elements connected by linear spring elements with stiffness values experimentally or theoretically determined. Concurrently, at the APS, an initiative has been undertaken to develop support and actuator systems that are standard and modular in design.[2] This initiative facilitates the design of new instrument support systems by utilizing a standard set of pre-designed components, such as actuators and couplings. Establishing a database of the mechanical vibratory properties of the standard components will provide valuable information when designing new systems for vibration stability. In addition, the mechanical vibratory information of common commercial devices is equally important. Currently, such databases do not exist but are under development for incorporation into an improved version of the vibratory modeling program of Basdogan.

DISCLAIMER

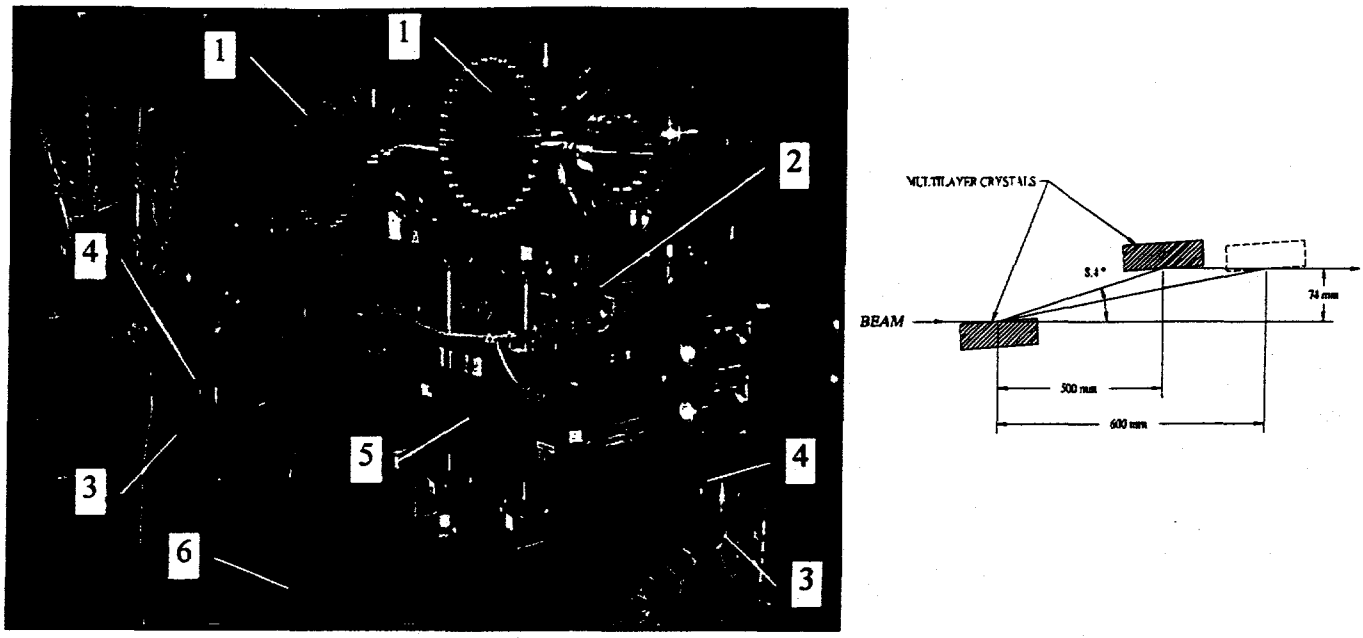

Figure 1. Double-multilayer monochromator (DMM) system: 1) crystal-housing vacuum chambers; 2) XZ stage; 3) 3-point kinematic mount stages; 4) self-aligning coupling; 5) middle frame; 6) truss frame

This paper presents the application of this modeling program to a double-multlayer monochromator (DMM) system,[3] shown in Figure 1. In synchrotron radiation facilities, such as the APS, monochromators are typically the first optical element on a beamline that accepts the full central-cone power of the radiation source.[4] Their primary purpose is the extraction of a specific band of energy from the broad radiation spectrum for various research programs including crystallography, spectroscopy, adsorption analysis, inelastic X-ray scattering, etc. Diffraction from a pair of crystals, the desired energy can be selected by adjusting their incident angle to the beam and by adjusting their relative spacing. The typical angular sensitivity needed to accomplish energy selection is on the order of microradians and must be performed by mechanical actuators. The design complexity of monochromators is affected by parameters such as desired energy bandwidth, crystal material, total power loading, power density, and X-ray beam size, and thus monochromators are designed for specific purposes. Figure 1 shows the current DMM system under study along with the optical schematic of the diffracting multilayer crystals.

2. MODELING PROGRAM

An earlier version of the vibration-modeling program presented here was developed and successfully applied to a high-precision optical table and mirror support system by Basdogan.[1] These two systems represent typical precision-motion systems having high stability requirements. Here, an improved version of the program is applied to the DMM system introduced above. Currently, the program determines the solution of a free, undamped, linear, multibody system connected with compliant elements, such as actuators, springs, and self-aligning couplings. The modal parameters that are determined from the solution are the natural frequencies and the corresponding mode shapes. The program produces a three-dimensional (3D) representation of the structure undergoing modal deformation. By applying the theory of multibody dynamics, the program's generic format permits the analysis of a system with any number of rigid bodies interconnected with compliant elements.

Figure 2 describes the steps involved in producing a theoretical model using the program. The first step is to generate a geometric model of the system. For each rigid body, a coordinate system is chosen that is consistent throughout the analysis. The theoretical information must then be determined regarding the mass, the mass-centroid, and the mass moments of inertia of each rigid body. Depending on the system's complexity, the geometric model information can be manually calculated. However, in complex systems without simple geometries, the use of 3D solid modeling software facilitates this step. In most cases, the systems to be analyzed are designed using this type of software, so that the geometric information is automatically available.

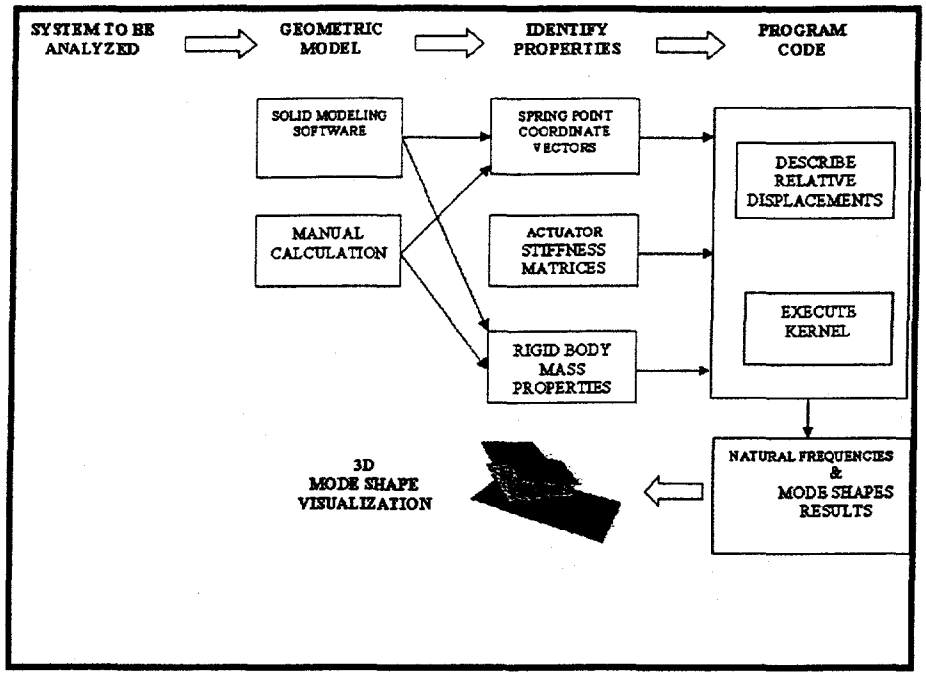

Figure 2. Program modeling process

Each rigid body's geometric properties are then identified in the program in matrix form. Thereafter, the mechanical properties of the compliant elements, such as actuators, are determined and identified in the program as 6 X 6 stiffness matrices. Currently, the program does not calculate the damped response, and thus the damping matrices are not required. The stiffness properties of the compliant elements, in some cases, can be analytically determined. Such cases include actuators with a simple compliant element, such as a beam or shaft that has deterministic compliant directions. In other cases, the mechanical properties must be measured experimentally because of assembly complexity, fastener joints, frictional forces, and inconsistency of any pre-loading forces.

The coordinate data identify the spring connection points between rigid bodies to the modeling program. In this step, vectors, defined in a rigid body's coordinate system, are attached to the body's center of mass and end at the spring connection point on the body. Once the mass properties, spring connection vectors, and stiffness matrices are defined, the relative displacement of each spring is formulated. This step identifies the coupling between rigid bodies and provides information to the global stiffness matrix.

Running the processing kernel calculates the eigenvalues and eigenvectors from which the system natural frequencies and mode shape parameters are known. A graphical representation of mode shapes is then plotted and displayed by the program.

3. THEORETICAL MODEL

3.1 Simplifications and Assumptions

In modeling real systems, the structure must first be analyzed to determine the source of major compliance. The compliance in the DMM structure primarily stems from the actuator and bearing elements that provide the positioning motions of the multilayer crystals. These include the 3-point kinematic mount stages, the self-aligning couplings, and the actuator/bearing elements comprising the XZ stage assembly. The other support elements, the base truss frame, the middle support frame, and the XZ stage frame, do not contribute to significant compliance in the frequency range of interest (<50 Hz) and are treated as rigid bodies. This assumption was verified experimentally. The rigid body assumption of the frames can also be determined beforehand utilizing finite element software.

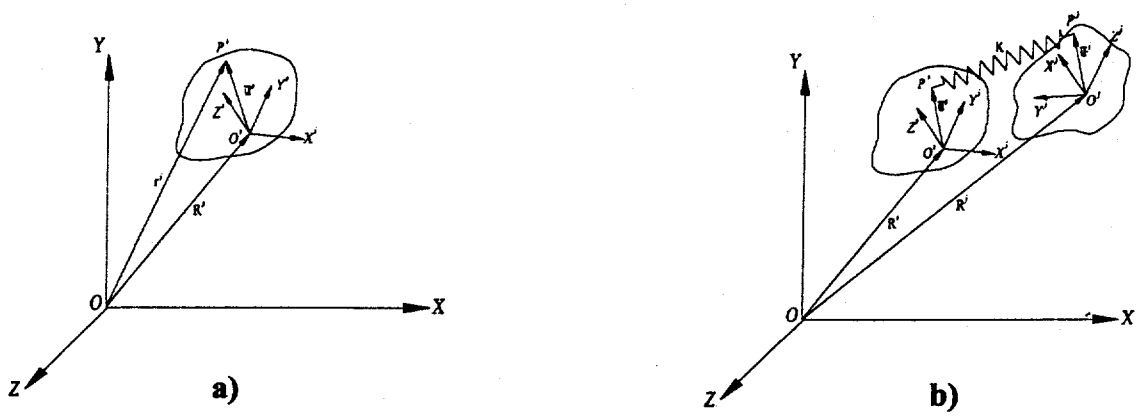

Figure 3. Kinematic description of a) a single rigid body, and b) a multibody system connected by a spring element.

Another consideration is the contribution of the actuators and bearing element masses to the overall response of the structure. In the analysis of the DMM support system, the masses of the vertical stages, the horizontal stages, and the self-aligning couplings that make up the 3-point pseudo-kinematic mount support are considered negligible. In addition, each mount comprising the 3-point kinematic support mount is treated as a lumped spring element. Thus for each mount, the stiffness definitions of the horizontal stage, the vertical stage, and the self-aligning coupling are combined using the traditional linear relationships for determining the equivalent spring rate of springs attached in series and/or in parallel.

Linear system theory is also assumed in the theoretical modeling of the DMM structure. This is valid because only very low amplitude vibratory motion is expected, resulting in negligible higher order displacement and rotation terms in the equations of motion. In addition, the spring elements in the structure are assumed linear for very small deflections about an operating point. Some of the elements that make up the kinematic mounts do not have linear stiffness behavior over the range of applied static loads. Examples of these are the cylindrical rolling bearings in the vertical stages and the ball bearing raceway interfaces in the self-aligning coupling assembly. For small dynamic perturbations about a static preload condition, the use of linear system theory is reasonable.[5]

3.2 Kinematics of Multibody Dynamics

The kinematic description of an unconstrained rigid body in space is given in terms of independent translation and rotation coordinates. Given a reference point on a rigid body with its local coordinate system fixed to this reference, the configuration of the body is defined by the translation of the reference point and by the rotation of the local coordinate system with respect to a global coordinate system. The rotation of the body in the global coordinate system is described using a 3 X 3 transformation matrix that depends on three orientation coordinates.

Figure 3a illustrates the kinematic description of a single, unconstrained rigid body in space. The global and local-body coordinate systems are given by XYZ and $X_iY_iZ_i$, respectively. The position vector of an arbitrary point P on this rigid body is given by the vector $\mathbf{r}^i$:

$$\mathbf{r}^i = \mathbf{R}^i + \mathbf{A}^i \bar{\mathbf{u}}^i \tag{1}$$

where $\mathbf{R}^i$ is the global position vector of the reference point O_i, $\mathbf{A}^i$ is the transformation matrix that defines the orientation of the body in the global coordinate system, and $\bar{\mathbf{u}}^i$ is a constant vector defining the location of the arbitrary point with respect to the body reference point.

3.3 Equations of Motion

Figure 3b illustrates a multibody system connected by a spring element. The number of degrees of freedom in a multibody system is equivalent to the number of independent coordinates required to describe the system. These coordinates are

referred to as generalized coordinates, and the number of independent generalized coordinates in a system of n_b unconstrained rigid bodies is equal to 6 X n_b. A vector **q** of the independent generalized coordinates is then defined as

$$\mathbf{q} = \begin{bmatrix} R_x^1 & R_y^1 & R_z^1 & \phi^1 & \theta^1 & \varphi^1 \ldots R_x^i & R_y^i & R_z^i & \phi^i & \theta^i & \varphi^i \ldots \\ \ldots R_x^{n_b} & R_y^{n_b} & R_z^{n_b} & \phi^{n_b} & \theta^{n_b} & \varphi^{n_b} \end{bmatrix}^T$$

$$= \begin{bmatrix} \mathbf{R}^{1T} & \theta^{1T} & \mathbf{R}^{iT} & \theta^{iT} \ldots \mathbf{R}^{n_b T} & \theta^{n_b T} \end{bmatrix}^T. \tag{2}$$

The dynamic equations of motion of a system of rigid bodies connected by spring elements and having the origin of the body coordinate system rigidly attached to the center of mass are written in matrix-partition form as[6]

$$\begin{bmatrix} \mathbf{m}^i_{RR} & \mathbf{0} \\ \mathbf{0} & \mathbf{m}^i_{\theta\theta} \end{bmatrix} \begin{bmatrix} \ddot{\mathbf{R}}^i \\ \ddot{\theta}^i \end{bmatrix} = \begin{bmatrix} (\mathbf{Q}^i_e)_R \\ (\mathbf{Q}^i_e)_\theta \end{bmatrix} + \begin{bmatrix} \mathbf{0} \\ (\mathbf{Q}^i_v)_\theta \end{bmatrix} \qquad i=1,2,\ldots,n_b, \tag{3}$$

where $\mathbf{R}^i$ and θ^i are the independent generalized coordinate vectors associated with the orthogonal translations R_x^i, R_y^i, R_z^i, and rotational translations ϕ^i, θ^i, φ^i, respectively, with each body denoted by *i*. The sub-matrices $\mathbf{m}^i_{RR}$ and $\mathbf{m}^i_{\theta\theta}$ are the mass matrices associated with the translation and orientation coordinates, respectively. $(\mathbf{Q}^i_v)_\theta$ is the centrifugal force vector, neglected in this work because very low angular velocities are expected. And, $(\mathbf{Q}^i_e)_R$ and $(\mathbf{Q}^i_e)_\theta$ are the vectors of generalized forces associated, respectively, with generalized translation and orientation coordinates. They are defined as

$$(\mathbf{Q}^i_e)_R = \sum_{j=1}^{n_f} \mathbf{F}^i_j \tag{4}$$

$$(\mathbf{Q}^i_e)_\theta = \mathbf{G}^{iT} \left[\sum_{j=1}^{n_m} \mathbf{M}^i_j + \sum_{k=1}^{n_f} (\mathbf{u}^i_k \times \mathbf{F}^i_k) \right], \tag{5}$$

where **F** and **M** are the forces and moments applied to the rigid body at point *i* on body *j*. These forces and moments also include the spring forces generated by the compliant elements, such as the positioning actuators and bearings. The generalized force and moment components of equations 4 and 5 can be developed for a set of rigid bodies that are connected by spring elements as shown in Figure 3b. Here, two rigid bodies are shown, denoted by *i* and *j*, and are connected by a spring with spring constant *k* at points P^i and P^j, respectively. The deformed and undeformed spring length is *l* and l_0, respectively. Thus, the spring force F_k that is acting between the two bodies acting along the line connecting points P^i and P^j is written as[6]

$$F_k = k(l - l_0), \tag{6}$$

where

$$l = \left| \mathbf{r}^{ij}_p \right| = \sqrt{\mathbf{r}^{ij\,T}_P \mathbf{r}^{ij}_p} \tag{7}$$

$$l_0 = \left| \mathbf{r}^{ij}_{p0} \right| = \sqrt{\mathbf{r}^{ij\,T}_{P0} \mathbf{r}^{ij}_{p0}}\,. \tag{8}$$

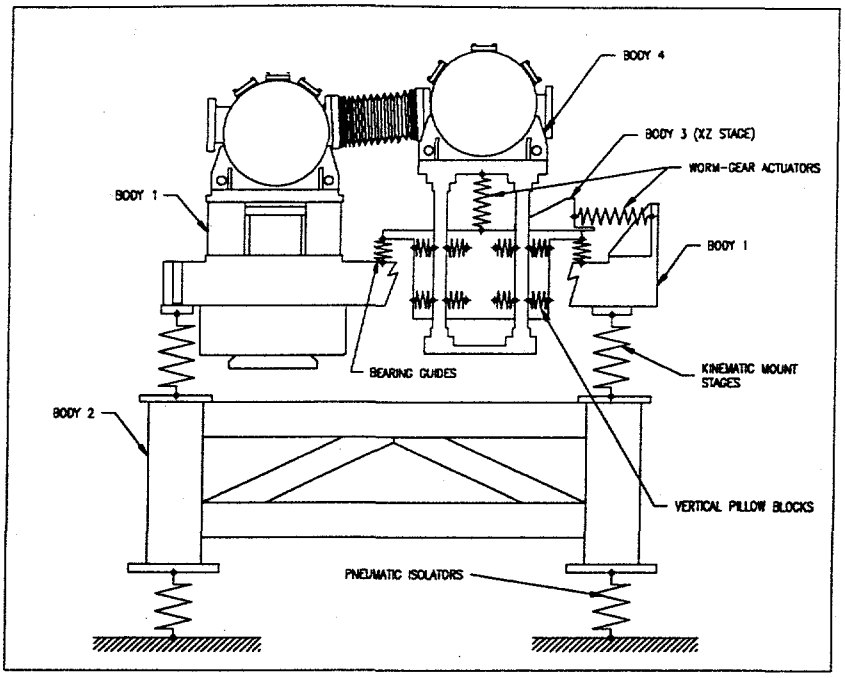

Figure 4. Multilayer monochromator theoretical model

The final and initial position vectors of the point P^i with respect to point P^j are $\mathbf{r}_p^{ij}$ and $\mathbf{r}_{p0}^{ij}$ and are given by

$$\mathbf{r}_P^{ij} = \mathbf{r}_p^i - \mathbf{r}_p^j = \mathbf{R}^i + \mathbf{A}^i \bar{\mathbf{u}}_P^i - \mathbf{R}^j - \mathbf{A}^j \bar{\mathbf{u}}_p^j \qquad (9)$$

$$\mathbf{r}_{P0}^{ij} = \mathbf{r}_{p0}^i - \mathbf{r}_{p0}^j \, .$$

The generalized force vectors in the right-hand side of Equation 3, with the exception of the centrifugal force vector, are functions of the linear spring constants that represent the actuators in the structure. For the undamped case, the equations of motion can be combined and represented in the more traditional form

$$\mathbf{M}\ddot{\mathbf{q}} + \mathbf{K}\mathbf{q} = \mathbf{0} \, . \qquad (10)$$

Equation 10 represents the governing equation of motion for the free-undamped case of multibody vibrations. **M** is the global mass matrix, **K** is the global stiffness matrix, and **q** is the generalized coordinate vector defined by Equation 2. Equation 10 can be evaluated to determine the natural frequencies and mode shapes of the monochromator system by applying the standard eigenvalue approach.[7] Figure 4 shows the theoretical depiction of the monochromator structure under investigation. This figure shows that the representation of the complex actuators and bearing components can be simplified to 3D linear spring elements connecting the rigid bodies. Earlier work by Basdogan[1] implemented the use of this simplification and was successful in modeling comparable high-precision optical systems. This work also neglected the inertial properties of the components that contribute to significant compliance in the system. As shown, the DMM theoretical model comprises four rigid bodies interconnected with a number of spring elements that represent stages, bearing guides, or worm-gear actuators. Note that the vacuum chambers are combined with their respective support body to form a single, larger body in the model. This assumption is valid because the interface between a support element and the vacuum chamber has negligible compliance. Also, for experimental purposes, the DMM was supported on pneumatic isolators to decouple the DMM structure from floor dynamics. These isolators were included as part of the theoretical model. The spring elements are 3×3 stiffness matrices in this model, neglecting the generalized forces that are associated with the rotational translations. This assumption is appropriate because, after evaluating each actuator, the actuators do not effectively transmit concentrated moment forces due to their incorporation of self-aligning rolling bearings.[5] However, the generic design of the modeling program still permits a full 6×6 stiffness definition for any actuator design.

4. EXPERIMENTAL MODEL

4.1 Experimental Modal Analysis

Typically, experimental modal analysis is performed on a structure with the goal of verifying and comparing analytical results or to determine the modal parameters of a structure that does not lend itself to a convenient analytical approach.[8] Several methodologies exist for implementing modal analysis, and choosing the correct one depends on the objective of the study.[9] A common objective is to study the structure undergoing vibration in its normal operating environment. A second objective, which is the one adopted here, is to study the response of the structure undergoing known excitations. The methodology in acquiring the modal parameters uses single input random force excitation from an electro-dynamic shaker while measuring the response from piezo-electric accelerometers. From the input and output digitized and scaled signals, the frequency response function (FRF) is calculated for each measurement point on the structure. Utilizing curve-fitting techniques to generate an analytical function from the FRF data, the resonant frequencies, damping, and residues can be estimated and used to plot the resulting modal deflection points on the structure. For multi-degrees of freedom (DOF), the frequency response transfer function is defined as

$$H_{ik}(\omega) = \sum_{r=1}^{n} \frac{A_{ikr}}{j\omega - p_r} + \frac{A_{ikr}^*}{j\omega - p_r^*}, \tag{11}$$

where i is the measured response DOF, k measured input DOF, r the modal vector number, A_{ikr} the residue, p_r is a system pole, and n is the number of modal frequencies.

4.2 Assumptions in Experimental Modal Analysis

Four basic assumptions are made on a structure undergoing experimental modal analysis for the frequency response transfer function to be valid. First, the structure is assumed to behave linearly, indicating that the response of the structure to any combination of forces is the sum of the individual responses of each force acting alone. In addition, the response level is linearly proportional to the input level. The second assumption requires that the structure be *time invariant*; i.e., the parameters that are to be determined by modal analysis are constants whose values do not depend on time. Third, *reciprocity* must be conformed to by the structure. Given a structure with an excitation at degree of freedom i that produces a response at degree of freedom k, by reciprocity, the response of the structure at degree of freedom i is the same if the excitation were applied at degree of freedom k. For the FRF this assumption is written as

$$H_{ik} = H_{ki}\,. \tag{12}$$

Finally, *observability* is required of the structure, implying that the complete measurement set must contain enough information to generate a behavioral model of the system. A non-observable system may have components that are not rigidly attached, resulting in missing data or data that describe an incomplete model of the system. More generally, a non-observable system has degrees of freedom that are not measured.

4.3 Experiment Model

Figure 5 highlights the measurement locations taken on the structure. Although the lower and middle frames are considered rigid in the modeling program, additional points were included along the frame beams to verify this assumption. The DMM assembly is supported on pneumatic bladders such that the floor stiffness and damping are uncoupled from the DMM structure. The structural frequency response up to 100 Hz is studied using random fixed excitation from an electrodynamic shaker while measuring the response from piezo-crystal accelerometers. All data were taken using a 16-channel DSP analyzer and were processed on commercial modal analysis software.

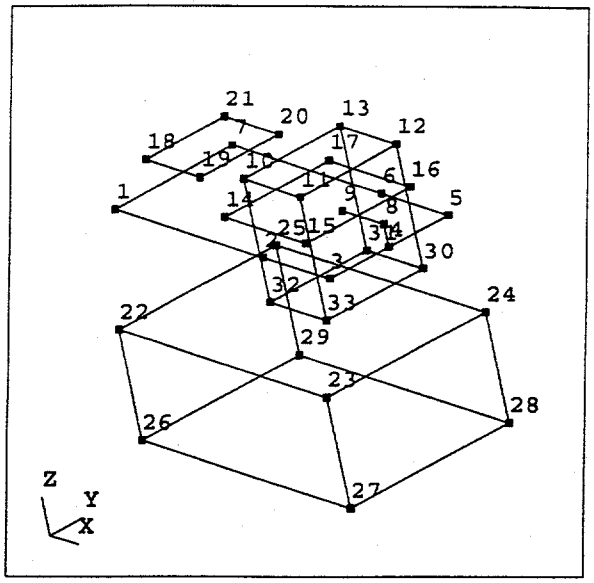

Figure 5. DMM measurement locations. Random excitation is applied at point 1 in the X, Y, Z directions.

5. RESULTS

5.1 Free-Undamped Response

A graphical representation of the DMM in its undeformed state is shown in Figure 6a. Each of the four planar surfaces represents a surface of each DMM body. Because the entire DMM assembly is supported on "soft" pneumatic bladders, it is possible to find all six rigid-body modes, both experimentally and theoretically. Applying the stiffness matrices for the bladders, the six rigid-body mode shapes were determined analytically, four of which are depicted in Figure 6c with their corresponding experimental result in Figure 6b. As shown, there is good agreement between the theoretically and experimentally determined rigid-body modes, demonstrating the effective use of pneumatic bladders for decoupling the floor dynamics.

Figure 7 compares the experimental and theoretical model results for selected natural frequencies below 50 Hz. The lowest non-rigid body mode is observed at 29.44 Hz. At this frequency, the XZ stage exhibits significant linear motion in the X direction and significant rotational motion about the Y-axis, which is verified experimentally at 23.33 Hz, indicating that the four-shaft guide bearings and the horizontal worm gear actuator have the highest compliance relative to other actuator elements. The top plate of the XZ stage, corresponding to the base of the second vacuum chamber, contributes primarily to the resonances at 37.58 Hz and 42.50 Hz, in agreement with experimental results. The last two mode shapes at 33.49 Hz and 52.88 Hz are associated with deflection of the kinematic mount positioning stages, which contributes to a full upper rigid body rotation about the Z axis and pure out-of-phase translation along the X axis. Note that the XZ stage exhibits significant translational and rotational motion even at 52.88 Hz. By observing the experimental results, it is clear that the system resonance's result from the actuators' compliance. Therefore, the rigid body modeling assumption for the structural elements is a correct one because no significant structural deformation is observed.

While the mode shapes agree very well with experimental results, the calculated natural frequencies only agree to within a few Hz. This slight disagreement could be due to various reasons. First, the actuator stiffness properties applied in the model may not exactly match the properties of the real actuator. This problem can be solved by statistically measuring the properties of several representative actuators and obtaining a uniform set of properties. Second, the load distribution (static load) on the actuators was not precisely used in determining their load-dependent stiffnesses; i.e., all three kinematic mount actuators were modeled with the same vertical stiffness. The stiffness of the actuators has some dependence on the applied load due to their design complexity; therefore, it is possible that each of the three kinematic mounts will have its own stiffness property. Third, each body mass property is not exactly determined. At the time of analysis, some components that are mounted inside the DMM vacuum chambers were not available for the solid modeling software; therefore, the lumped mass properties may not exactly match those of the real system.

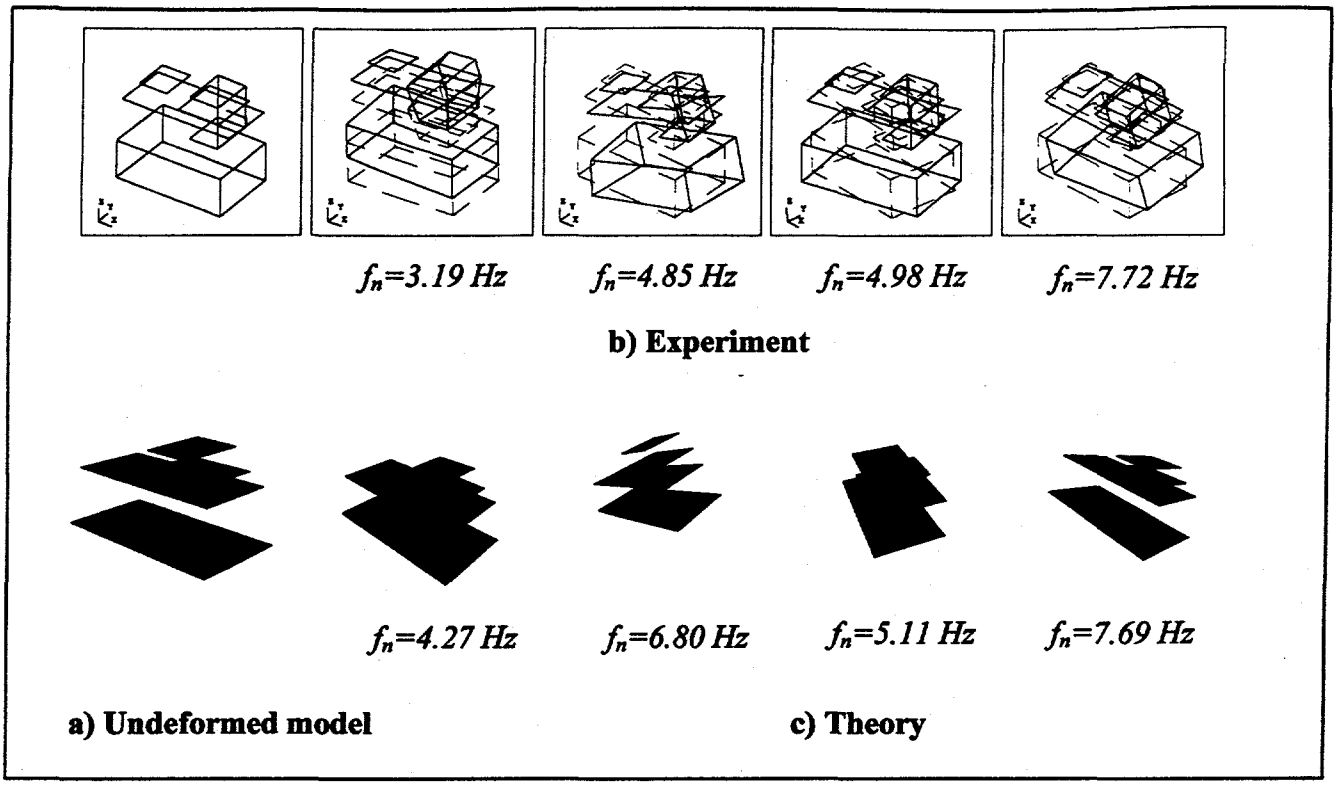

Figure 6. Selected rigid body mode shapes

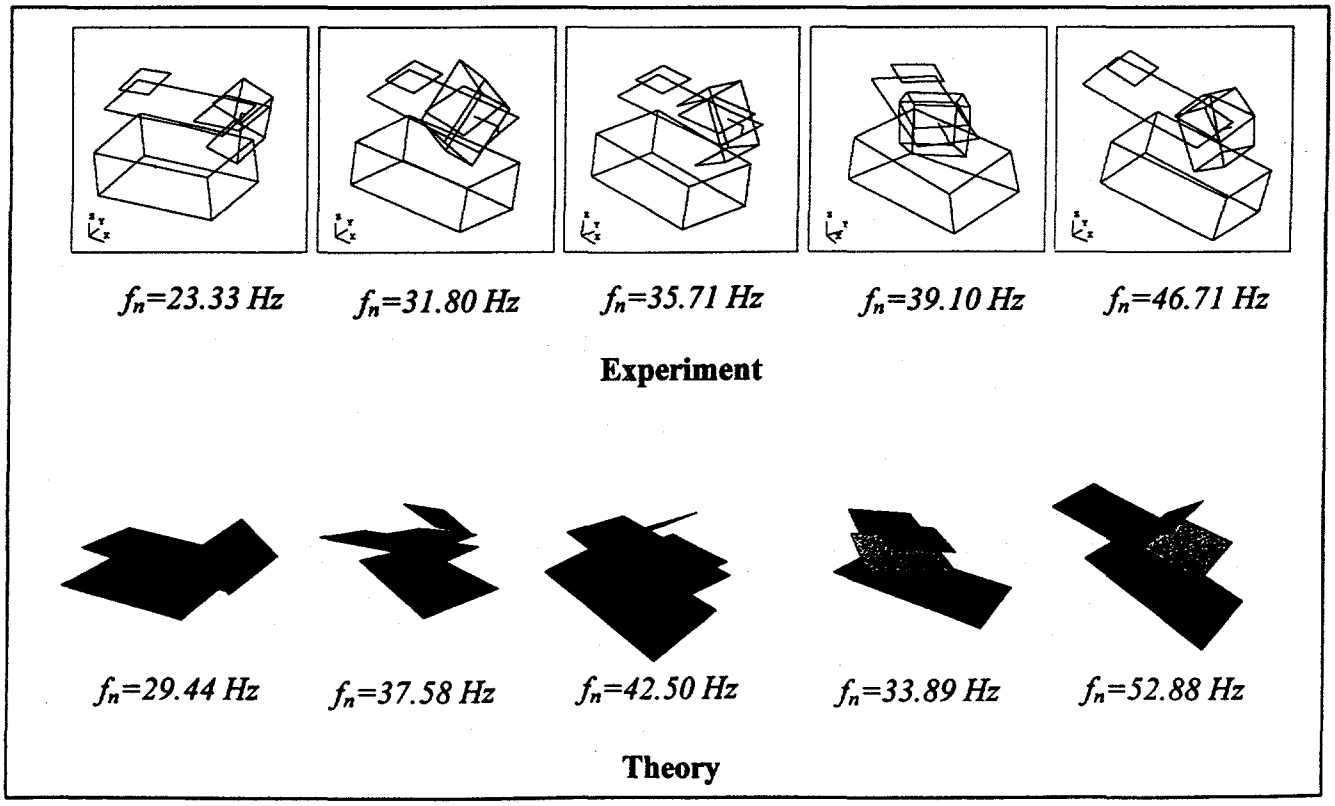

Figure 7. Comparison of theoretical and experimental modal analysis results.

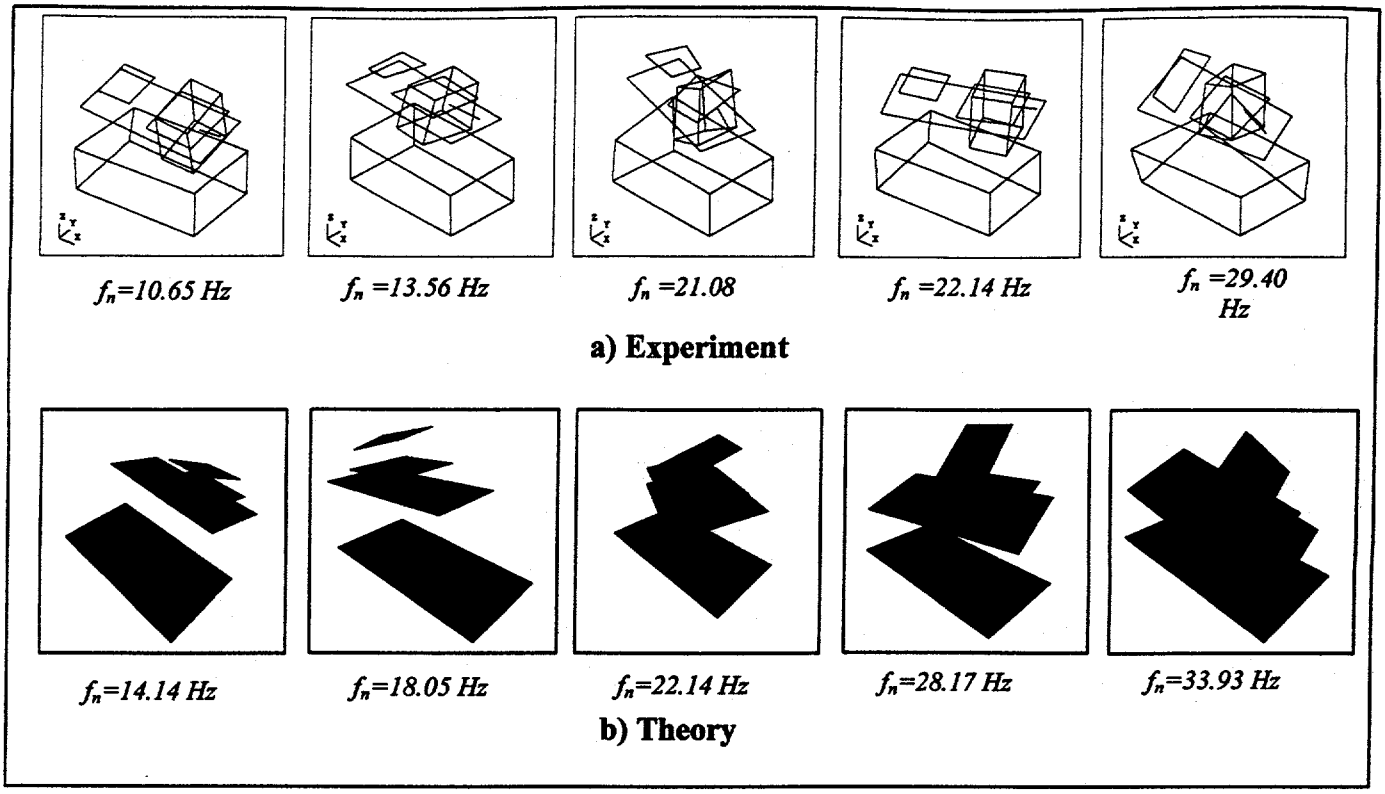

Figure 8. Comparison of theoretical and experimental case study results.

5.2 Case Study

The DMM was modeled as a free-floating structure in space with a relatively "soft" interaction, provided by the pneumatic isolators, between the laboratory floor and the base frame. Although this is satisfactory from an analytical standpoint, the design engineer is also interested in the DMM's vibratory behavior in the actual operating environment. To this end, the modeling program was modified to simulate actual operating conditions, that is, with the DMM bolted to the experiment floor on the beamline. This modeling was accomplished by changing the spring stiffness definition of the pneumatic isolators to a value several orders of magnitude greater, essentially making them noncompliant

The lowest five natural frequencies of the bolted-down simulation results are shown in Figure 8. The first four mode shape deflections indicate that the primary source of compliance stems from the kinematic mount actuators between the base frame and the upper DMM assembly. These mode shapes occur at much lower frequencies compared to the "floating" case scenarios. Upper rigid-body translation and rotations occur at the lowest four modes, while the lifting portion of the XZ stage exhibits significant deflection at 33.93 Hz.

The drop in natural frequency as indicated by the low values (14.14 Hz, 18.05 Hz, 22.14 Hz, and 28.17 Hz) that results from the bolted-down simulation is an inherent effect of multiple-body vibrating systems. To gain fundamental insight, the base frame and upper assembly of the DMM system can be modeled as a simple two-body, spring-mass system, as shown in Figure 9. Therefore, the natural frequency of the deflection mode shape can be determined for the floating and for the bolted-down configuration by adjusting the value of the spring stiffness k_1, representing the pneumatic bladders. In Figure 9a, the masses of the base frame and the upper DMM assembly are represented by m_1 and m_2, respectively. The spring stiffness of the kinematic mount actuators is given by k_2. A parametric study of this system revealed that the deflection mode frequency response of a free undamped system is always higher than the frequency response of a grounded system. (The 2-body system of Figure 9 is grounded by increasing the stiffness value of k_1.) The plot in Figure 9b shows the results of this parametric study and indicates that, as the m_2/m_1 ratio increases from zero, the ratio of the natural frequency response of the free configuration to the natural frequency response of the bolted-down configuration is always greater than 1

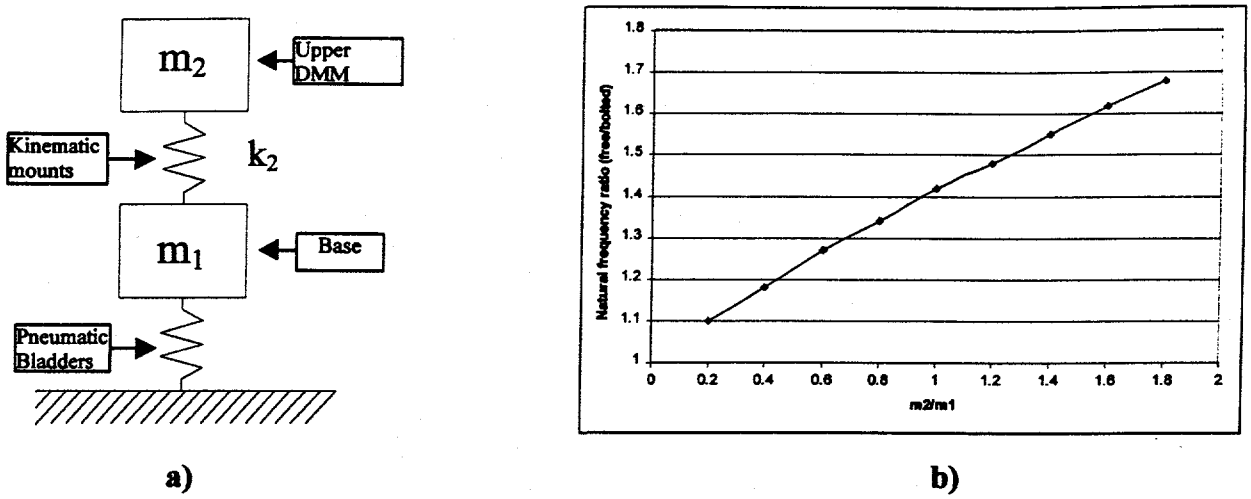

a) b)

Figure 9. a) Simplified 2-body spring-mass system. b) Parametric study results.

.The principal concern in this case study result is the significant natural frequency reduction of the primary deflection mode shapes that stem from the 3-point kinematic mount actuators. The goal of a positioning system design at the APS is to achieve high frequency response above the lowest characteristic natural frequency, between 6.7 Hz and 7.6 Hz,[10] at the APS site. Although the DMM bolted-down condition results in frequencies that are close to the experimental floor dynamics, the DMM system performance is not expected to be adversely affected, because the amplitude levels of the experimental floor vibrations are on the order of 10's of nanometers in most places and the floor motion is relatively uniform throughout the APS. However, disturbances from local water pumping systems or rotating motors nearby may excite the low frequency modes on the DMM, affecting the intensity and position of the monochromatic X-ray beam that the DMM produces.

6. CONCLUSIONS

This study investigated the application and experimental verification of a generic vibratory modeling program to determine the vibratory response of a high-precision, double-multilayer monochromator. Based on the theory of multibody dynamics, the modeling program was designed with a generic algorithm. As such, systems with different rigid-body configurations and numbers, and different actuator and bearing designs, can be modeled by updating the program mass property matrices and the coordinate vectors to the actuator and bearing connection points. The program then calculates the modal parameters, that is, the free and undamped natural frequencies and mode shapes, of the DMM and presents the results in a 3D form. Although all the natural frequencies are calculated in the DMM structure, the number corresponding to the degrees of freedom in the formulation, this study focused only on frequencies less than 50 Hz. In this study, the DMM system is assumed to follow linear system theory. This assumption is reasonable given the low vibratory amplitude motions that are expected.

This program allows the design engineer to accurately assess the rigidity of a structure, based on the natural frequencies and mode shapes, during the design process, where undesirable vibratory behavior can be corrected before committing to manufacturing. Presently at the APS, these precision optical support systems are designed with the empirical knowledge and experience of the design engineer. Thus, this work can result in more efficient and economical future designs. In addition, this program can also be implemented to identify the actuator specifications; that is, by using an iterative process, the actuator stiffness properties can be identified to gain the most optimum system performance. It is also possible to build a property database of common actuators, which have been experimentally verified, as a tool for analyzing other complex optical systems during the design phase. This work is in progress. Additionally, the program will be upgraded to include the actuator damping properties, as well as response to input excitation, with the end goal of determining vibratory amplitudes.

7. ACKNOWLEDGEMENTS

This work is supported by the U.S. Department of Energy, Office of Science, under contract no. W-31-109-ENG-38.

8. REFERENCES

1. I. Basdogan, " A theoretcial and experimental study of the dynamic response of high precision optical positioning systems," Ph.D. Dissertation, Department of Mechanical Engineering, University of Illinois at Chicago, 1997.
2. D. Shu, J. Barraza, C. Brite, J. Chang, T. Sanchez, V. Tcheskidov, T.M. Kuzay, "Beamline standard component designs for the Advanced Photon Source," *Review of Scientific Instruments* 66 (2), 1795-1797 (1995).
3. Shu, D., Yun, W., B. Lai, J. Barraza, and T.M. Kuzay, "Double-multilayer monchromator using a modular design for the Advanced Photon Source," *Review of Scientific Instruments* 66 (2), 1786-1788 (1995).
4. L.E.Berman, Z. Yin, S.B. Dierker, E. Dufresne, S.G.J. Mochrie, O.K.C. Tsui, S.K. Burley, F. Shu, X.Xie, M.S. Capel, and R.M. Sweet, "Performance of the double multilayer monochromator on the NSLS wiggler beam line X25," *Synchrotron Radiation Instrumentation*: Tenth US National Conference, American Institute of Physics Conference Proceedings 417, 1997.
5. Royston, T.J. and I. Basdogan, "Vibration transmission through self-aligning (spherical) rolling element bearings: Theory and experiment," *Journal of Sound and Vibration* **215** (5), 997 – 1014 (1998).
6. Shabana A.A., *Computational Dynamics*, New York, Springer Verlag, 1994.
7. Shabana A.A., *Theory of Vibration*, Volume 2, New York, Springer Verlag, 1991.
8. Harris, C.M., *Shock and Vibration Handbook*, New York, McGraw-Hill, 1961.
9. Ewins, D.J., *Modal Testing: Theory and Practice*, New York, John Wiley & Sons, 1984.
10. J.A. Jendrzejczyk, M.W. Wambsganss, and R.K. Smith, "Dynamic response of the APS Storage Ring Basemat: Preliminary Measurements," Argonne National Laboratory report APS/IN/VIB/92-5, June 1992.